ОБЪЕДИНЕННЫЙ
ИНСТИТУТ
ЯДЕРНЫХ
ИССЛЕДОВАНИЙ

JOINT
INSTITUTE
FOR NUCLEAR
RESEARCH

Москва, Главпочтамт п/я 79

Head Post Office, P.O. Box 79, Moscow USSR

МЕЖДУНАРОДНАЯ КОНФЕРЕНЦИЯ ПО ФИЗИКЕ ВЫСОКИХ ЭНЕРГИЙ

Дубна 5 - 15 августа 1964 г.

THE 1964 INTERNATIONAL CONFERENCE ON HIGH ENERGY PHYSICS

Dubna, August 5 - 15.

ДОКЛАДЫ РАППОРТЕРОВ RAPPORTEURS' REVIEWS

E-1790

STRANGE PARTICLE PHYSICS
(Experimental)

Rapporteur: D.H. Miller

Secretaries: N.M. Viryasov
V.G. Ivanov
E.V.Kusnetsov

Дубна 1964

E-1790

STRANGE PARTICLE PHYSICS
(Experimental)

Rapporteur: D.H. Miller

Secretaries: N.M. Viryasov
V.G. Ivanov
E.V. Kusnetsov

This publication is of a preliminary character. To facilitate the rapid appearance of Reports, they are printed in the form as presented by Rapporteurs.

A wide variety of painstakingly acquired experimental information has been presented during the sessions on Strange Particle Physics. Because of space limitations, it is possible in some cases to discuss only typical examples to illustrate a particular point.

I. Properties of the Baryon Octet.

A. Hyperon Magnetic Moment.

A new measurement of the Λ magnetic moment has been reported by Gibson et al. (Bristol, Geneve, Lausanne, Munich Collaboration). The experimental arrangement is shown in Fig.1. The Λ's resulted from associated production by $1.07 + 0.02$ GeV/c π^- mesons incident on a polyethelene target. In contrast to previous experiments, emulsion stacks oriented with their planes parallel to the initial polarization of the Λ's were used as detectors. Before entering the emulsions, the Λ's travelled through 11 cm of a pulsed transverse magnetic field of abour 150 kgauss, so that the decay pattern rotated about the normal to the emulsion plane. Thus far, 109 Λ events have been found which satisfy a set of criteria imposed to ensure good measurement and minimum contamination of the sample. The analysis was performed on 65 of these events observed in a region of low background in the emulsion stacks.

The maximum likelihood fit to the decay distribution is shown in Fig.2. The best estimate for the Λ magnetic moment is

$$\mu_\Lambda = -0.5 + 0.3$$

in units of nuclear magnetons. In Table I this value is compared with those obtained in previous experiments. In the limit of exact SU_3 symmetry, but to first order in electromagnetism, Coleman and Glashow (Phys. Rev. Letters 6, 423 (1961) have shown that $\mu_\Lambda = 1/2\mu_n$ (= -0.96).

The limited experimental data available do not yet permit a quantitative check of this prediction. However, it is important to note that a comparison of μ_{Σ^+} and μ_p provides a stronger test of SU_3 since the prediction of equality is valid to all orders in the electromagnetic interaction.

B. Masses.

Several groups have attempted to improve the mass determinations using the hyperons produced by absorption of K^- mesons stopped in a hydrogen bubble chamber. The results of these measurements are summarized in Table II.

Each group has made rather different use of the available experimental data. Burnstein et al. (Phys. Rev. Letters 13, 66 (1964)) used a range-momentum relation as calibrated from measurement of stopping $\pi^+ \to \mu^+$ decays together with the accepted K, π, and Σ^+ masses. This approach resulted in an internally consistent set of data. Dosch et al. (Heidelberg) used the relative $\pi^\mp$ momenta in the $\Sigma^\pm \pi^\mp$ events to determine $M_{\Sigma^-} - M_{\Sigma^+}$. Both groups used $\Sigma^- + p \to e^+ + e^- + \Lambda + n$ events to calculate $M_{\Sigma^-} - M_{\Sigma^0}$ In the work of Schmidt et al. (Columbia-Rutgers Collaboration), an attempt was made to fit all the K^-p absorption reactions simultaneously using the hydrogen density, magnetic field, and baryon masses as free parameters. A poor fit is obtained unless reactions depending upon range measurements are supressed. However, when this is done serious disagreements exist in the Λ and Σ^- masses. When the range measurements are included, the same Σ^- mass is obtained as by Burnstein et al. Investigation of the source of the discrepancy continues.

It should be noted that all groups agree that the mass splittings within the Σ triplet are not symmetric. The values may be compared with the predictions of Coleman and Schnitzer, $M_{\Sigma^-} - M_{\Sigma^0} \simeq 5.8$ Mev, and $M_{\Sigma^0} - M_{\Sigma^+} \simeq 3.8$ MeV, reported at another session of the Conference.

II. Low-Momentum Hyperon-Nucleon Scattering.

The same film has been used to measure the cross-sections for hyperon-nucleon scattering.

A. Λ-p Scattering

Alexander et al. (Rehovoth-CERN Collaboration) observed 58 events satisfying a predetermined set of selection criteria and lying in the momentum interval 120-320 MeV/c. Sechi-Zorn et al. (University of Maryland) obtained 75 events with somewhat similar selection criteria. Their data are shown in Fig.3. The dashed and solid curves illustrate the cutoffs for two different selection criteria. Within statistics, the angular distributions observed by both groups were isotropic in the interval accepted. In each experiment, a measurement of an unbiased sample of Λ's together with appropriate scaling to the entire sample provided the path length as a function of momentum. The combined results are shown in Fig.4.

The theoretical curve represents an effective-range calculation using the parameters for the singlet and triplet states suggested by De Swart and Dullemond (Annals of Physics 19, 458 (1962)) from an analysis of hyperfragment data: $a_s = -3.6f$, $r_s = 2f$, $a_t = -0.53f$, and $r_t = 5f$.

B. $\Sigma^+ p$ and $\Sigma^- p$ Interactions.

The Maryland and Heidelberg groups have also studied the $\Sigma^+ p$ and $\Sigma^- p$ interactions. The details of the experiments are similar and results are summarized in Table III. All cross-sections were calculated assuming that the distributions were isotropic outside the Coulomb interference region.

Two important points may be noted:

(a) SU_3 predicts that $\sigma(\Sigma^+ p) = \sigma(pp)$. Because of the Pauli principle only the singlet states may be compared. At the same CM momentum, $\sigma(p,p)$ = 165 mb. Consequently, if SU_3 is valid, the triplet $\Sigma^+ p$ interaction must be weak.

(b) The $\Sigma^- p$ absorptive reaction is very strong, with the data suggesting considerable p-wave ($\sigma_{abs.} > \pi \lambda\!\!\!^{-2}$) even at the low momenta studied.

III. $K^- p$ Interactions at Higher Momenta.

A. The Reaction $K^- p \rightarrow \Lambda \eta$ near Threshold.

Berley et al. (BNL) have studied $\Lambda \eta$ production at four momenta just above the η threshold (approximately 720 MeV/c). The observed cross-section (neutral plus charged modes) rises sharply immediately above the η threshold and falls off rapidly with increasing momentum. The data are shown in Fig.5. A somewhat similar behavior has been reported by Bastien et al. (MIT) and Peterson et al. (Berkeley-Hawaii Collaboration) for the reaction $\pi^- + p \rightarrow \eta n$ at another session.

This marked energy dependence has been interpreted in terms of the K-matrix formalism of Dalitz and Tuan (Annals of Physics 3, 307 (1960)), considering only the channels

$$K^- + p \rightarrow K^- + p \qquad \text{(a)}$$

$$K^- + p \rightarrow \Lambda + \eta \qquad \text{(b)}$$

and

$$\Lambda + \eta \rightarrow \Lambda + \eta \qquad \text{(c)}$$

Since the CM K^- momentum varies little over the range studied, the K-matrix may be parameterized in terms of the $\Lambda\eta$ scattering length: $a = c + i\,d$. A fit to the data indicates that $d \ll |c|$ and $3 \lesssim |c| \lesssim 20$f. If $c < 0$, a bound state of $\Lambda\eta$ may be expected at $\sim$ 2 MeV below threshold, decaying predominantly into $\Sigma\pi$. Unfortunately, the presence of $Y_1(1660)$ complicates the search for such decays.

Since the authors have interpreted the effect as a result of a strong S-wave interaction, we may assume that the angular distribution is consistent with isotropy. Consequently, it does not appear likely that this peak can represent an $I = 0$ state associated with a $J = 3/2^-$ unitary multiplet.

B. Two-Particle Final States above 1 GeV/c.

Several detailed studies of elastic and charge-exchange scattering in the region 1.3-3.5 GeV/c have been presented. Although a great deal of evidence for structure is observed, thus far it has not been possible to do more than fit the angular distributions in terms of powers of cos Θ. However, the importance of additional accurate charge-exchange data in identifying possible resonant states is neatly demonstrated in Fig.6, from the report by Barbaro-Galtieri and Tripp (Berkeley). Strong peaks in the total cross-section are observed at Y_0^* (1520) and Y_0^* (1815).

Fits to the $\Sigma^{\pm}\pi^{\mp}$ and $\Lambda\pi^0$ final states in the 1 - 2 GeV/c momentum interval also reveal little as to the nature of the structure present. However, at 3.5 GeV/c, Haque et al. (British Collaboration) estimate that $\sigma(\Sigma^+\pi^-)/\sigma(\Sigma^-\pi^+) \sim 12$. In addition, the Σ^+ 's are peaked sharply in the backward direction, indicating that the region dominated by peripheral interactions in this final state has been reached.

C. Multiparticle States with a Λ or $\Sigma^{\pm}$

Analyses of multiparticle final states with a Λ or $\Sigma^{\pm}$ illustrate the importance of resonance production at higher momenta. As a typical example we show in Fig.7 the effective-masses for the $\Lambda\pi^+\pi^0\pi^-$ final state at 2.45 GeV/c as discussed by Ross et al. (Berkeley). Clearly, a study of the production mechanisms in such a state represents a complicated and challenging task.

As a second example, we show the effective-mass distributions in Fig.8 for the $\Sigma^{\pm}\pi^{\mp}\pi^+\pi^-$ final states at 2.63 and 2.70 GeV/c presented by Ficenec et al. (Illinois-Berkeley Collaboration). Again the complexity of the final state is apparent.

In summary, the most important general feature of the K^-p data presented is the tendency for dominance of resonance production through peripheral processes with increasing momentum. Only those charge states are produced copiously which are accessible through exchange of I = 0, 1/2, or 1 systems; angular distributions are characteristic of processes involving exchange of low-mass systems.

D. Production of Ξ^- -Hyperons.

The cross-sections for Ξ^- production in 2,3,4,5 and 6 body final states have been summarized by Barnes et al. (BNL-Syracuse Collaboration) for K^- momenta to 5 GeV/c. The data are given in Fig.9. Analyses of the final states by many groups have shown that Ξ^- 's observed in multiparticle final states are either produced in association with a K^*, or result from decay of S = -2 baryon resonant states.

E. Production and Decay of the Ω^-

A further search by Barnes et al. (BNL group) for Ω^-'s produced in 5 GeV/c K^-p interactions has yielded no new unambiguous candidates over the original two. Extensive study of the fitting procedures confirms their interpretation as valid Ω^- events. From the sample size and branching ratios (only for the decay modes observed) they correspond to a cross-section of ~ 2 μb. A study of the errors gives the following best estimate for the masses:

Event 1:	Revised to	1677 + 9 MeV(a)
Event 2:		1674 + 3 MeV(b)
Average :		1675 + 3 MeV.

(a) V.E. Barnes et al., Phys. Rev. Letters 12, 204 (1964)

(b) V.E. Barnes et al., Sumbitted to Phys. Letters.

IV. Strange Particle Production in $\bar{p}$ - p Interactions at 6.74 GeV/c.

The production of strange particles in $\bar{p}$ - p interactions at 6.94 GeV/c has been investigated by Baltay et al. (Yale-BNL Collaboration). The $\bar{\Lambda}-\Lambda$ final state is shown in Fig.10, The angular distribution shows a stronger peaking than at 3.69 GeV/c, consistent with an exchange model. In addition, the $\Sigma^+\bar{\Sigma}^-$, $\Sigma^+\bar{\Lambda}\pi^-$, and $\bar{\Sigma}^-\Lambda\pi^+$ final states together with their charge conjugates were examined for consistency with the K or K^* exchange model. In all cases, the $Y(\bar{Y})$ or $Y^*(\bar{Y}^*)$ charge states observed could be produced through exchange of $I = 1/2$, $S = -1$ systems. Similar results were obtained in a study of 5.7 GeV/c $\bar{p} - p$ interactions reported by R. Bock et al. (CERN-Saclay Collaboration).

Baltay et al. also carried out a systematic search for events which might be Ω^- or its charge conjugate. No event with a satisfactory fit to any expected Ω^- decay mode was observed. Taking into account the path length and detection efficiency, the upper limit for Ω^- production is $\sim 3\mu b$ for an Ω^- lifetime of $\sim 2 \times 10^{-10}$ sec.

V. Strange Particle Production in p - p Interactions at 5.5 GeV/c.

Alexander et al. (Rehovoth) have studied p - p interactions at 5.5 GeV/c leading to final states involving either a Λ or K^0. For the three-body final states $\Lambda p K^+$, $\Sigma^0 p K^+$ and $\Sigma^+ p K^0$ the data suggest that YK systems result from excitation and subsequent decay of $N^*(1688)$ and $N^*(1920)$. The effective-mass combinations for the four-body final states $\Lambda K N\pi$ and $\Sigma^0 K N\pi$ are shown in Fig.11. Strong enhancements are observed at $N^*(1238)$ and $Y^*(1385)$. The baryon angular distributions in all cases are consistent with the dominance of peripheral interactions.

Similarly, the extensive studies of $\pi^- p$ interactions at 3 - 4 GeV/c presented by Brannik et al. (Dubna-Bucharest Collaboration) and Hardy et al. (Berkeley) again emphasize the increasing importance at higher momenta of resonance production in peripheral collisions. Consequently, the qualitative understanding of much of the data presented was based upon the exchange model. The question remains as to the possibility that these reactions can be described quantitatively by this model.

VI. Discussion of the Exchange Model.

The most detailed attempts to fit the peripheral model have been carried out in the analysis of K^+ interactions. Ferro-Luzzi et al. (CERN) have extended their study of the reaction $K^+p \rightarrow K^0 p \pi^+$ from 3.0 to 3.5 GeV/c, with qualitatively similar results (an earlier report is given in Phys. Letters 9, 359 (1964)). The $p\pi^+$ mass distribution for their latest 3.0 GeV data is shown in Fig.12; the $K^0\pi^+$ mass spectrum in Fig.13. It is clear that the reaction proceeds through either the $K N^*$ (1238) or $N K^*$(888) intermediate state. We shall discuss only the $N K^*$ events in this report. The Δ^2 distribution to the K^*'s is given in Fig.14. The peak at low Δ^2 is again characteristic of an exchange mechanism.

The angular distribution for the K^* decay in its CM is most conveniently parameterized in terms of the elements of the density matrix, ρ_{ij} Choosing the z-axis of quantization along the direction of the incident K^+, and the x-axis in the production plane, the decay distribution is given by

$$W(\theta,\phi)d\Omega = \frac{3}{4\pi}\left[\rho_{00}\cos^2\theta + \frac{1}{2}(1-\rho_{00})\sin^2\theta - \rho_{1,-1}\sin^2\theta\cdot\cos 2\phi - \sqrt{2}\,\mathrm{Re}\,\rho_{1,0}\sin 2\theta\cdot\cos\phi\right]d\Omega$$

For the two simplest cases of interest it is readily shown that:

(a) exchange of a pseudoscalar meson yields an angular

distribution $\propto \cos^2\theta$, so that $\rho_{00}=1$, and $\rho_{1,-1}=\rho_{1,0}=0$;
and

(b) for vector meson exchange $\rho_{00}=0$

The angular distributions for the K^* decay at 3.0 GeV/c are shown in Fig. 15. Clearly, the reaction is dominated by exchange of a vector meson. However, in order to account for the Δ^2 dependence, it would be necessary to arbitrarily introduce a form factor with a strong dependence on Δ^2 . Such a form factor would be in contradiction with other knowledge of nuclear structure, implying and unacceptably large radius of interaction at each vertex. In an effort to overcome this objection, Gottfried, Jackson, and Svensson (to be published) along with others have developed a model which attempts to take into account the absorptive processes in the low partial waves. This results in a strong collimation in the forward direction and a non-zero value for ρ_{00} even for pure vector meson exchange. The elements of the density matrix also assume a dependence on Δ^2 .

An interesting test of the model may be provided by a comparison of the reactions.

$$K^+ + p \rightarrow K^{*+} + p \qquad (a)$$

and

$$K^- + p \rightarrow K^{*-} + p \qquad (b)$$

since the absorptive processes in the initial and final states should be different in the two cases.

A detailed study of reaction (b) has been presented by the Amsterdam-Ecole Polytechmique_Saclay Collaboration. A comparison of results is shown in Table IV. The agreement appears better than expected if absorptive processes rather than form factors actually produce the additional forward collimation.

However, detailed evaluation of the model has not yet been carried out for this case.

It is interesting to note that since a proton appears in the initial and final states, neither of the reactions discussed distinguishes between ρ and ω or ϕ exchange.

A study of K^+d interactions has been reported by Goldhaber et al. (Berkeley). They have examined the reactions

$$K^+ + p(n) \rightarrow K^{*+} + p(n) \qquad (c)$$

and

$$K^+ + n(p) \rightarrow K^{*0} + p(p) \qquad (d)$$

The Dalitz plots are shown in Fig. 16. The K^* bands are clearly distinguished. The decay angular distributions are given in Fig. 17. As discussed above, reaction (c) is dominated by vector meson exchange, and yields the characteristic $\sin^2\theta$ decay distribution with respect to the incident K^+ direction. However, the distribution for (d) contains a large $\cos^2\theta$ component, consistent with a strong contribution from pion exchange. The corresponding marked difference in Δ^2 dependence is shown in Fig. 18.

Since the π and ρ have the same isospin, their relative contributions to the two reactions must be the same. Consequently, we conclude that the vector meson exchange has $I = 0$.

As a final example, we mention the study of $K^+p \rightarrow K^+\pi^-p\pi^+$ at 3.5 GeV/c presented by Grard et al. (Brussels). The scatter plot in Fig. 19 indicates that the reaction proceeds mostly through the K^* N^* (1238) intermediate state. The Δ^2 distribution to the K^* is shown in Fig. 20. Again the peripheral nature of the process is apparent. In Fig. 21, a plot of the density matrix elements is given for three intervals of Δ^2 .

The large value for ρ_{00} at low Δ^2 indicates the dominance of pion exchange. The non-zero values for the other elements can be attributed to a small admixture of vector meson exchange or to modifications of the density matrix through absorptive processes.

It may be expected that during the next year an adequate amount of quantitative data will become available over both a large range of incident energies and a wide variety of final states so that detailed tests can be made of the theoretical models currently being suggested for description of the exchange process.

Received by Publishing Department on August 17, 1964.

Table I

Summary of measured values of Λ magnetic moment.

Experimenters	Detector	μ_Λ
R.L. Cool et al.[a]	Spark chamber	-1.5 ± 0.5
W. Kernar et al.[b]	Diffusion cloud Chamber	0 ± 0.6
T. Anderson and F. Crawford [c]	Hydrogen bubble Chamber	-1.3 ± 0.7
W.M. Gibson et al.	Emulsion	-0.5 ± 0.3

(a) R.L. Cool et al., Phys. Rev. 127, 2223 (1962)

(b) W. Kernan et al., Phys. Rev. 129, 870 (1963)

(c) J.A. Anderson and F.C. Crawford, Bull. Am. Phys. Soc. 9, 459 (1964)

Table II

Summary of hyperon masses as determined in hydrogen bubble chamber

	R.A. Burnstein et al. (a)	H.G. Dosch *et al.*	P. Schmidt et al without range	P. Schmidt et al with range	Theory[+]
M_Λ	1115.36 ± 0.14*		1115.86 ± 0.08		
M_{Σ^-}	1197.0 ± 0.2		1197.53 ± 0.10	1196.80±0.26	
M_{Σ^0}	1192.25 ± 0.23		1192.47 ± 0.12		
M_{Σ^+}	1189.4 ± 0.2*		1189.60 ± 0.10	1190.144±0.19	
$M_{\Sigma^-}-M_{\Sigma^0}$	4.75 ± 0.10	4.87±0.12	5.00 ± 0.12		5.8±1
$M_{\Sigma^0}-M_{\Sigma^+}$	2.85 ± 0.30	3.43±0.32	2.96 ± 0.16		3.8±1
$M_{\Sigma^-}-M_{\Sigma^+}$	7.6 ± 0.28	8.3 ±0.25	7.96 ± 0.10		

(a) R.A. Burnstein et al. Phys. Rev. Letters 13, 66 (1964)

*Input data. The K^- mass in taken as 493.9 ± 0.2 and $\pi^\pm$ mass as 139.56 MeV.

+Coleman and Schnitzer (this Conference).

Table III

SUMMARY OF CROSS-SECTIONS FOR Σ^+ AND Σ^- INTERACTIONS FOR AN AVERAGE MOMENTUM OF 150 + 10 MeV/c

$\pi \lambda\!\!\!^{-2} \simeq 295$ mb

	R.A. Burnstein et al.	H.G. Dosch et al.		Average
$\Sigma^+ p \rightarrow \Sigma^+ p$	$= 160 \pm 60$ mb	$= 185 \pm 55$ mb		$= 174 \pm 41$ mb
$\Sigma^- p \rightarrow \Sigma^- p$	$= 200 \pm 43$ mb	$= 232 \pm 82$		$= 215 \pm 32$
$\Sigma^- p \rightarrow \begin{pmatrix}\Lambda \\ \Sigma^0\end{pmatrix} + n$	$= 463 \pm 73$ mb	$= 450 \pm 100$ mb		$= 459 \pm 59$
$\frac{\Sigma^0}{\Sigma^0 + \Lambda}$ (in flight)	$= 0.57 \pm 0.10$			
$\frac{\Sigma^0}{\Sigma^0 + \Lambda}$ (at rest)	$= 0.44 \pm 0.03$	$0.39 \pm .03$		0.41 ± 0.2*

* Includes value 0.35 ± 0.06 obtained by Ross et al, Bull. Am. Phys. Soc. 3, 355 (1959)

T a b l e IV

Elements of density matrix and cross-sectionsfor

reactioøns $K^{\pm}+p \;\; K^{*\pm}+p$ at 3 GeV/c

	K^+	K^-
$\sigma_{tot}(K^0 p \pi^{\pm})$	2.1 ± 0.3 mb	1.49 ± 0.30 mb
$\sigma_{K^* p}$ $\hookrightarrow K^0 \pi$	0.8 ± 0.1	0.76 ± 0.15
Δ^2 (63%)	0.5 $(GeV/c)^2$	0.5 $(GeV/c)^2$
ρ_{00}	0.11 ± 0.05	0.17 ± 0.05
$\rho_{1,-1}$	0.34 ± 0.04	0.29 ± 0.04
$Re\,\rho_{1,0}$	-0.05 ± 0.04	0.01 ± 0.02

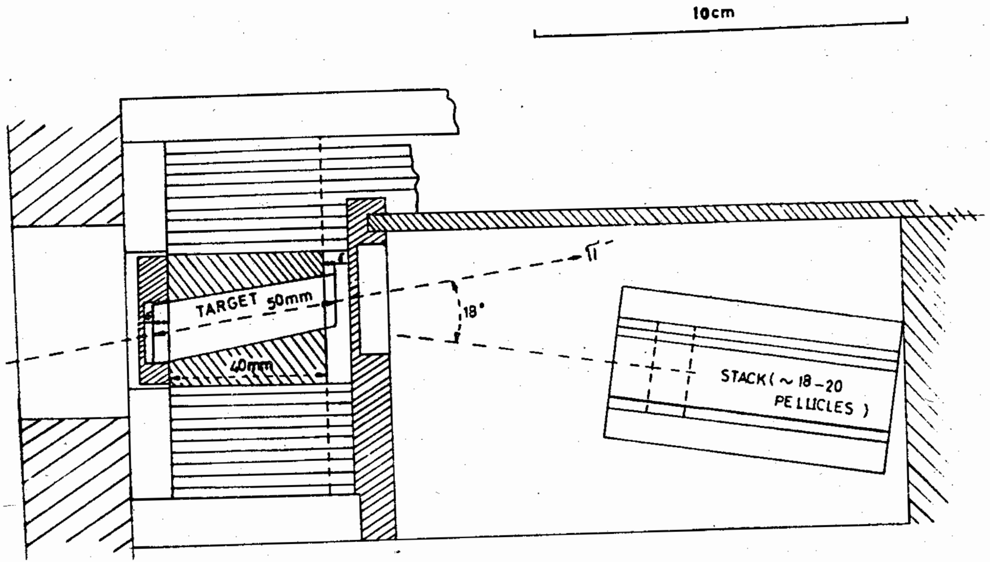

Fig.1.

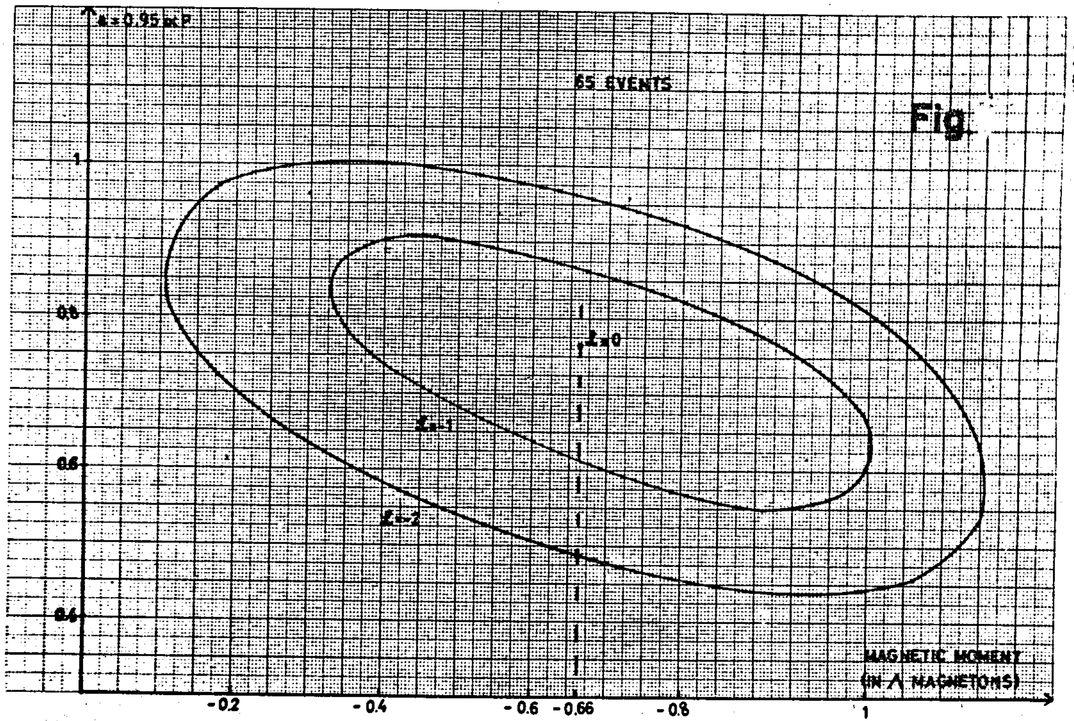
0.95
65 EVENTS
Fig.
1
0.8
0.6
0.4
-0.2
-0.4
-0.6
-0.66
-0.8
1
MAGNETIC MOMENT
(IN Λ MAGNETONS)

Fig.2.

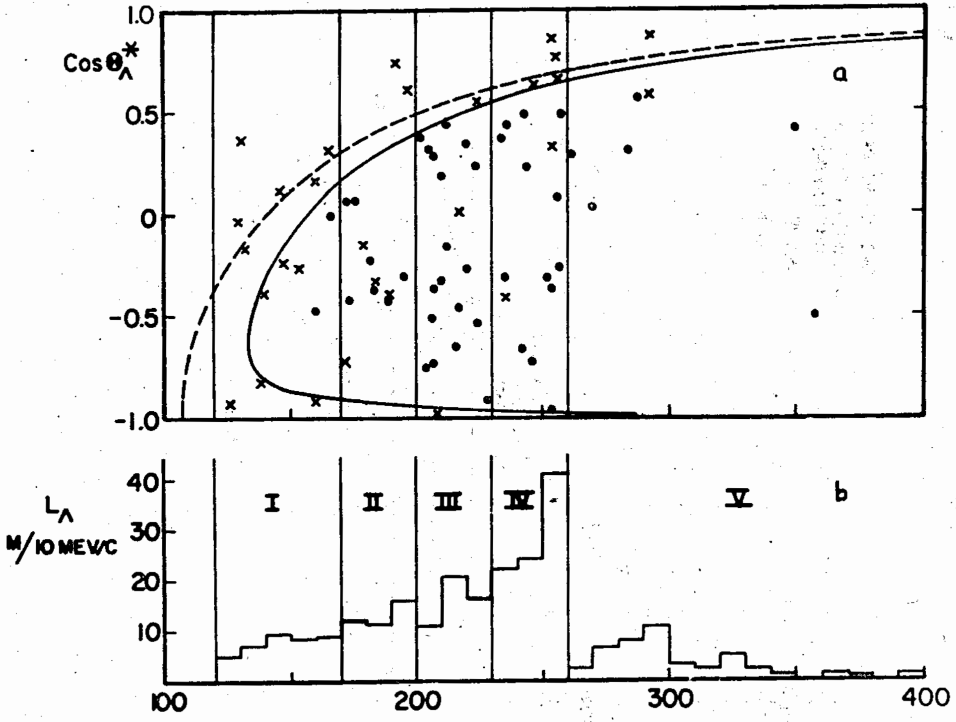

1.0
0.5
0
-0.5
-1.0
Cos θ*Λ
a
40
30
20
10
LΛ
M/10 MEV/C
I
II
III
IV
V
b
100
200
300
400

Fig.3.

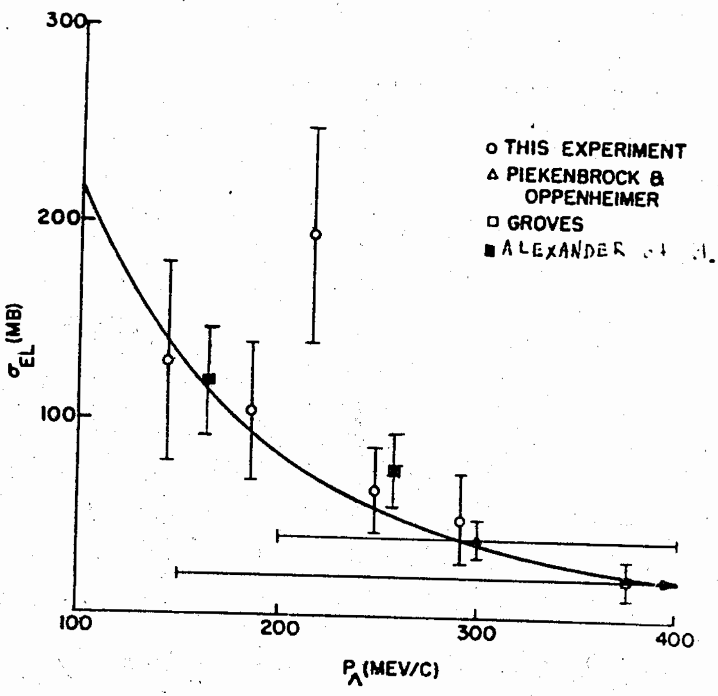

300
200
100
σ_{EL} (MB)
o THIS EXPERIMENT
△ PIEKENBROCK & OPPENHEIMER
□ GROVES
■ ALEXANDER
100
200
300
400
P_Λ (MEV/C)

Fig.4.

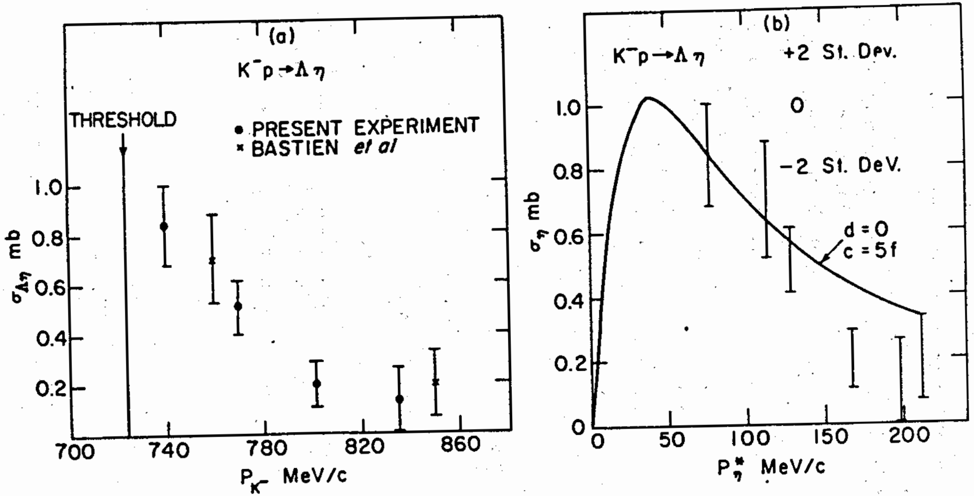

(a)
K⁻p → Λ η
THRESHOLD
• PRESENT EXPERIMENT
× BASTIEN et al
1.0
0.8
0.6
0.4
0.2
σ_Λη mb
700
740
780
820
860
P_K⁻ MeV/c
(b)
K⁻p → Λ η
+2 St. Dev.
0
−2 St. Dev.
d = 0
c = 5 f
1.0
0.8
0.6
0.4
0.2
0
σ_η mb
0
50
100
150
200
P*_η MeV/c

Fig.5.

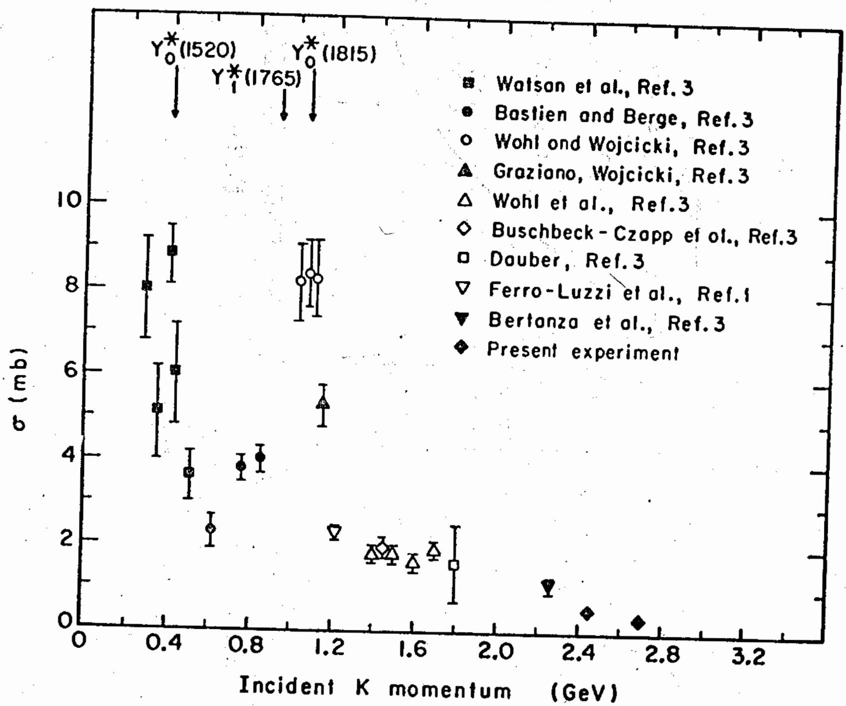

MUB-3444

Fig.6.

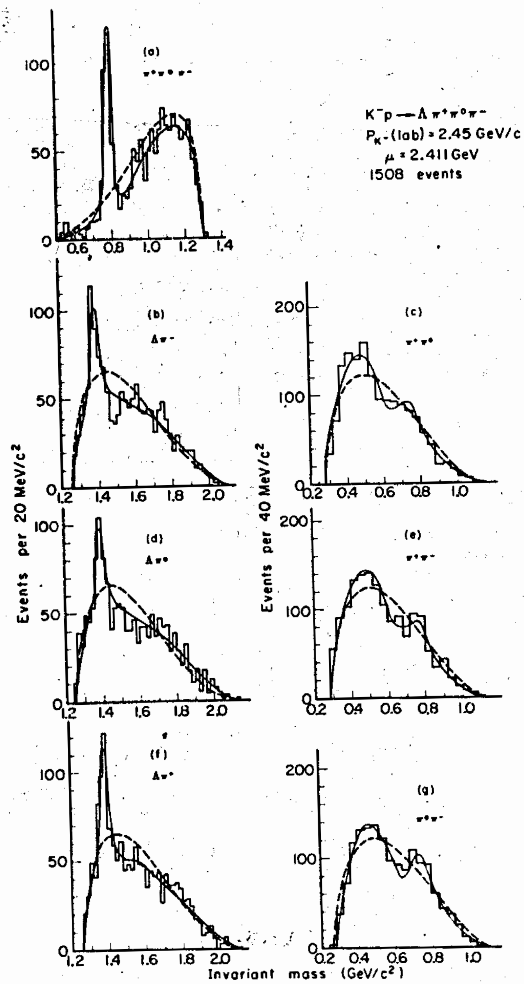

(a)
$\pi^+\pi^0\pi^-$
$K^-p \to \Lambda\pi^+\pi^0\pi^-$
P_{K^-}(lab) = 2.45 GeV/c
μ = 2.411 GeV
1508 events
(b)
$\Lambda\pi^-$
(c)
$\pi^+\pi^0$
(d)
$\Lambda\pi^0$
(e)
$\pi^+\pi^-$
(f)
$\Lambda\pi^+$
(g)
$\pi^0\pi^-$
Events per 20 MeV/c²
Events per 40 MeV/c²
Invariant mass (GeV/c²)

Fig.7.

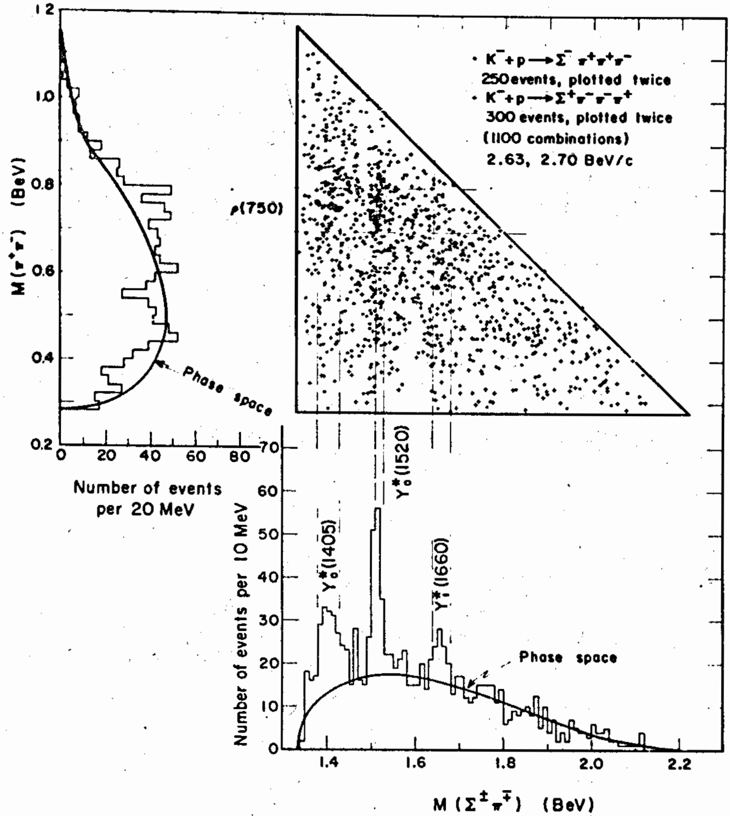
K⁻+p ⟶ Σ⁻π⁺π⁺π⁻
250 events, plotted twice
K⁻+p ⟶ Σ⁺π⁻π⁻π⁺
300 events, plotted twice
(1100 combinations)
2.63, 2.70 BeV/c
ρ(750)
M(π⁺π⁻) (BeV)
Phase space
Number of events per 20 MeV
Number of events per 10 MeV
Y*₀(1405)
Y*₀(1520)
Y*₁(1660)
Phase space
M (Σ±π∓) (BeV)

Fig.8.

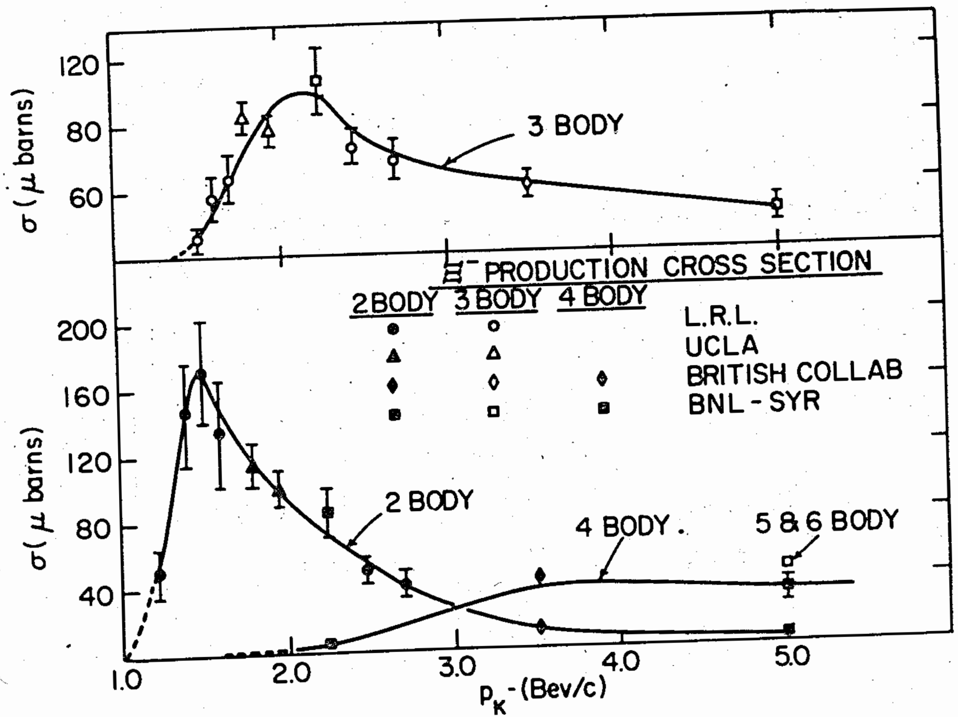

120
80
60
σ (μ barns)
3 BODY
Ξ⁻ PRODUCTION CROSS SECTION
2 BODY
3 BODY
4 BODY
L.R.L.
UCLA
BRITISH COLLAB
BNL - SYR
200
160
120
80
40
σ (μ barns)
2 BODY
4 BODY
5 & 6 BODY
1.0
2.0
3.0
4.0
5.0
p_{K^-} (Bev/c)

Fig.9.

Angular Distribution $\bar{p}+p \rightarrow \bar{\Lambda}+\Lambda$

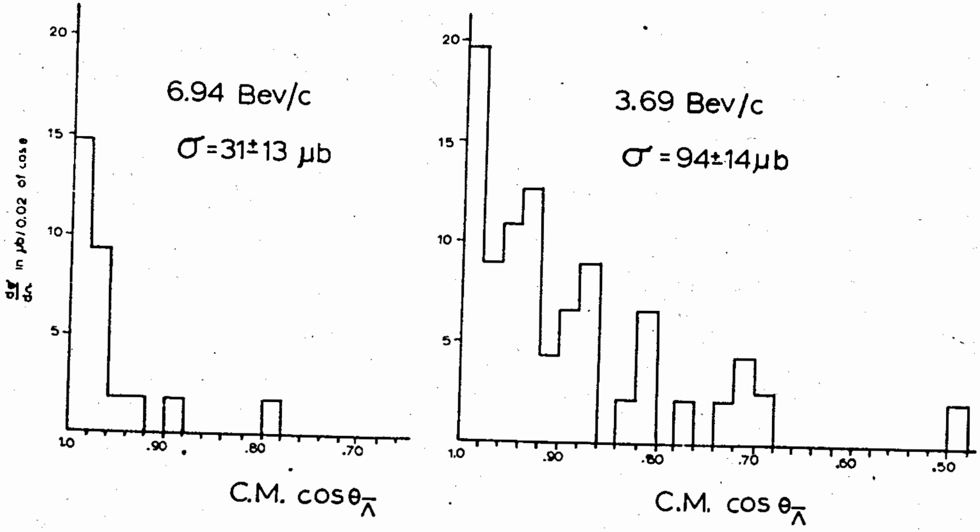

Fig.10.

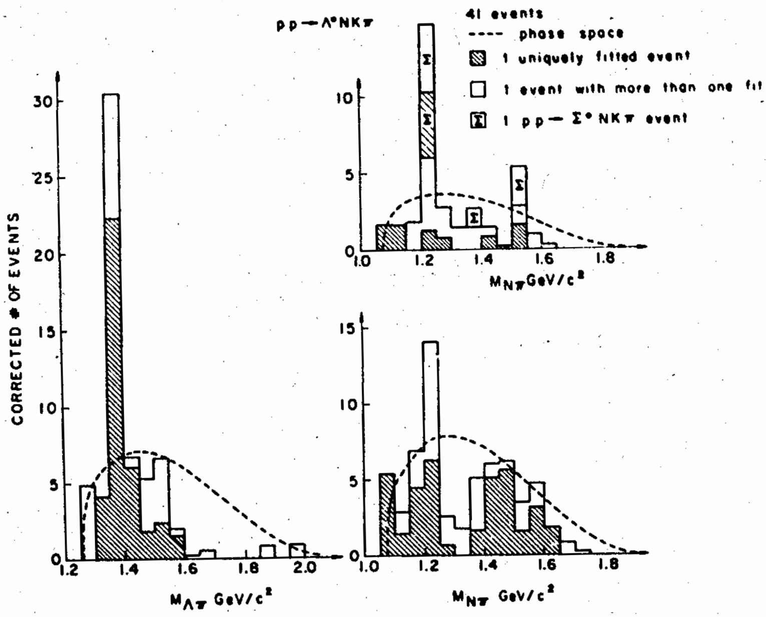

pp → Λ°NKπ
41 events
---- phase space
1 uniquely fitted event
1 event with more than one fit
1 pp → Σ° NKπ event
CORRECTED # OF EVENTS
M Λπ GeV/c²
M Nπ GeV/c²

Fig.11.

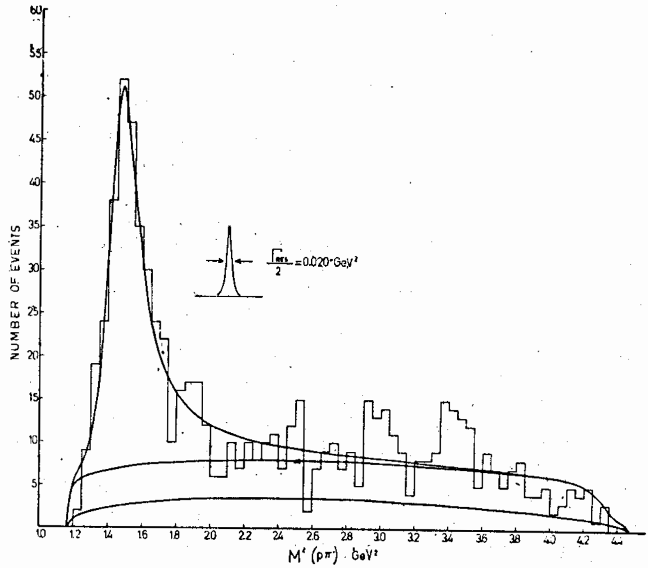
NUMBER OF EVENTS
$\frac{\Gamma_{res}}{2}$ = 0.020 GeV²
M² (pπ⁺) GeV²

Fig.12.

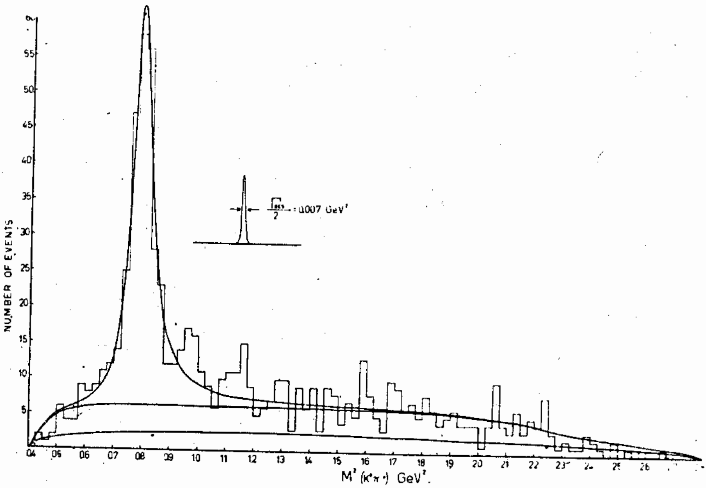
NUMBER OF EVENTS
M² (K⁺π⁺) GeV²

Fig.13.

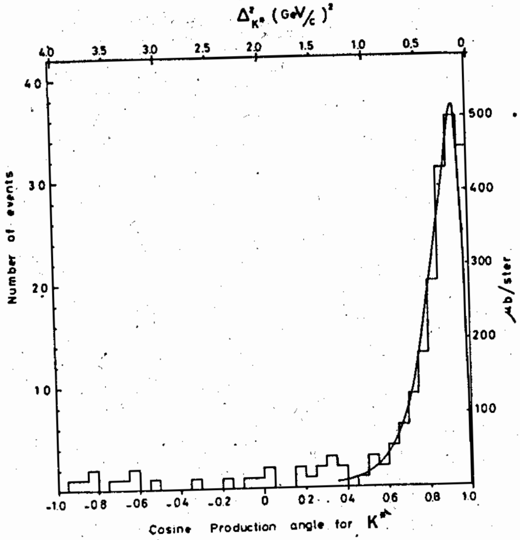

$\Delta^2_{K^*}$ (GeV/c)^2
4.0 3.5 3.0 2.5 2.0 1.5 1.0 0.5 0
40 30 20 10
Number of events
500 400 300 200 100
μb/ster
-1.0 -0.8 -0.6 -0.4 -0.2 0 0.2 0.4 0.6 0.8 1.0
Cosine Production angle for K^*

Fig.14.

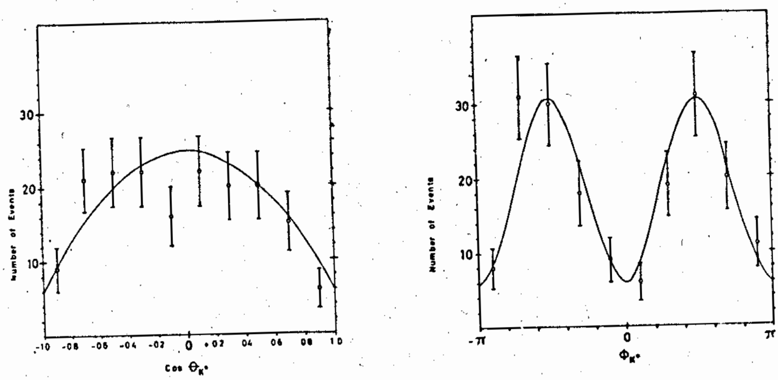

30 20 10
Number of Events
-1.0 -0.8 -0.6 -0.4 -0.2 0 +0.2 0.4 0.6 0.8 1.0
Cos Θ_{K^*}
30 20 10
Number of Events
-π 0 π
Φ_{K^*}

Fig.15.

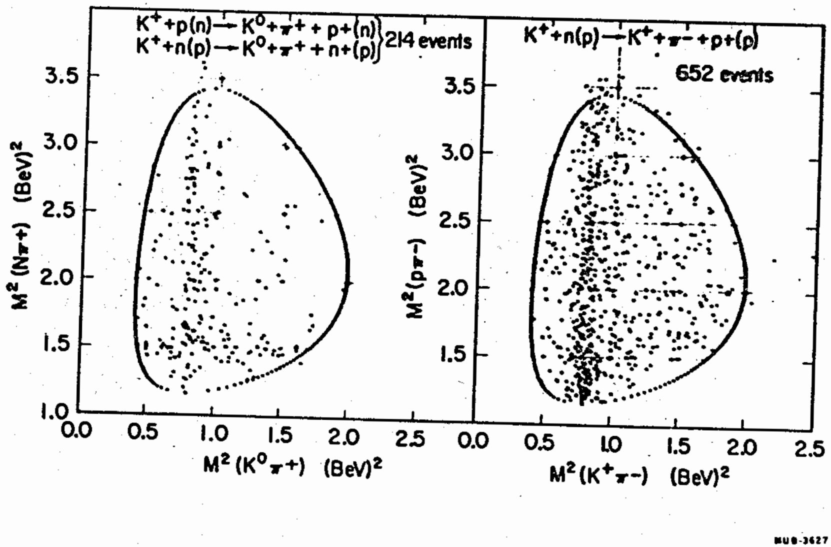
K⁺+p(n)→K⁰+π⁺+p+(n)
K⁺+n(p)→K⁰+π⁺+n+(p)
214 events
M² (Nπ+) (BeV)²
M² (K⁰π+) (BeV)²
K⁺+n(p)→K⁺+π⁻+p+(p)
652 events
M²(pπ-) (BeV)²
M²(K⁺π-) (BeV)²
MUB-3627

Fig.16.

Distribution in the scattering angle in the (Kπ) system

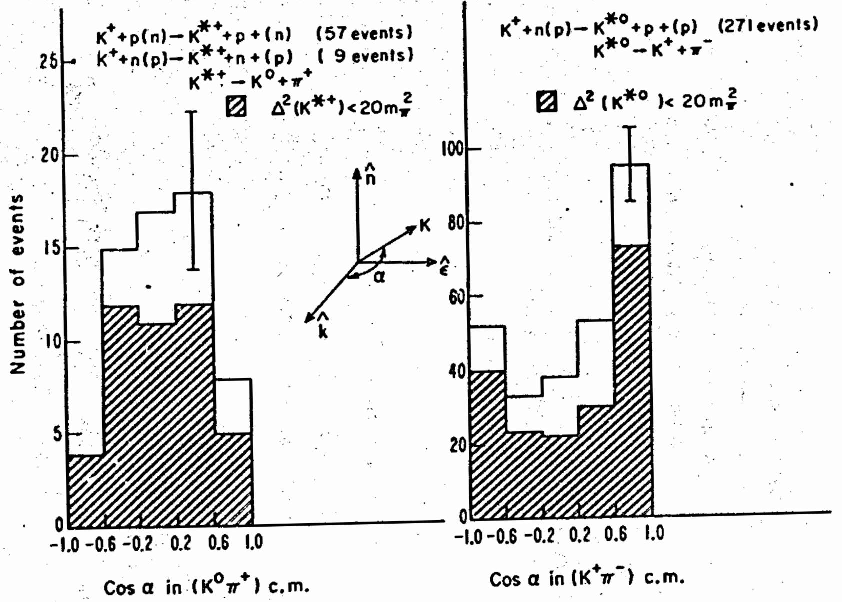

MUB-3625

Fig.17.

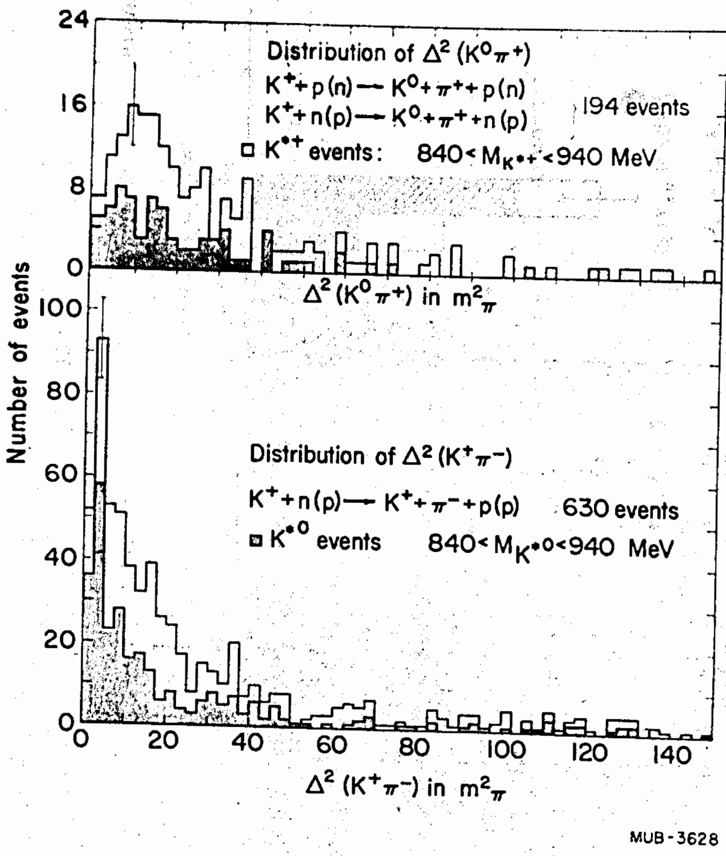
Distribution of Δ² (K⁰π⁺)
K⁺+p(n) → K⁰+π⁺+p(n)
K⁺+n(p) → K⁰+π⁺+n(p)
194 events
K*⁺ events: 840 < M_K*⁺ < 940 MeV
Δ² (K⁰π⁺) in m²_π
Number of events
Distribution of Δ² (K⁺π⁻)
K⁺+n(p) → K⁺+π⁻+p(p)
630 events
K*⁰ events 840 < M_K*⁰ < 940 MeV
Δ² (K⁺π⁻) in m²_π
MUB-3628

Fig.18.

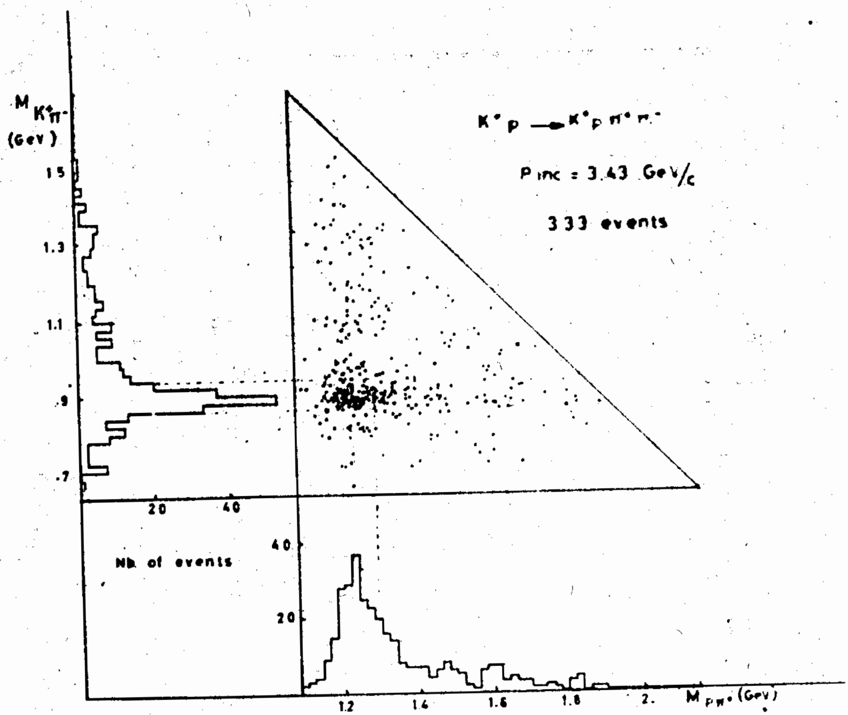

$M_{K^+\pi^-}$
(GeV)
1.5
1.3
1.1
.9
.7
20
40
Nb. of events
K⁺p ⟶ K⁺p π⁺ π⁻
P inc = 3.43 GeV/c
333 events
40
20
1.2
1.4
1.6
1.8
2.
M pπ⁺ (GeV)

Fig.19.

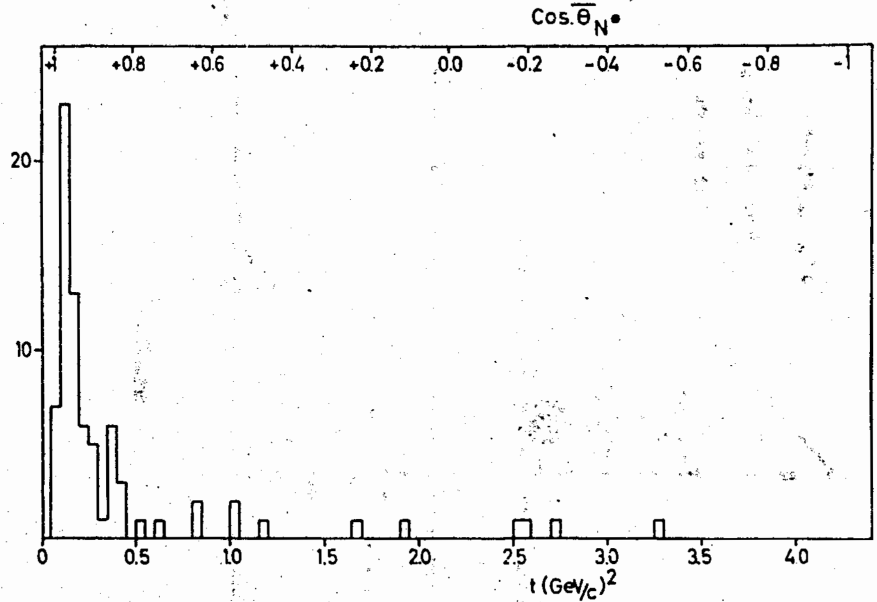

Momentum transfer distribution for K^* in $K^* N^*$ events (77events)

Fig.20.

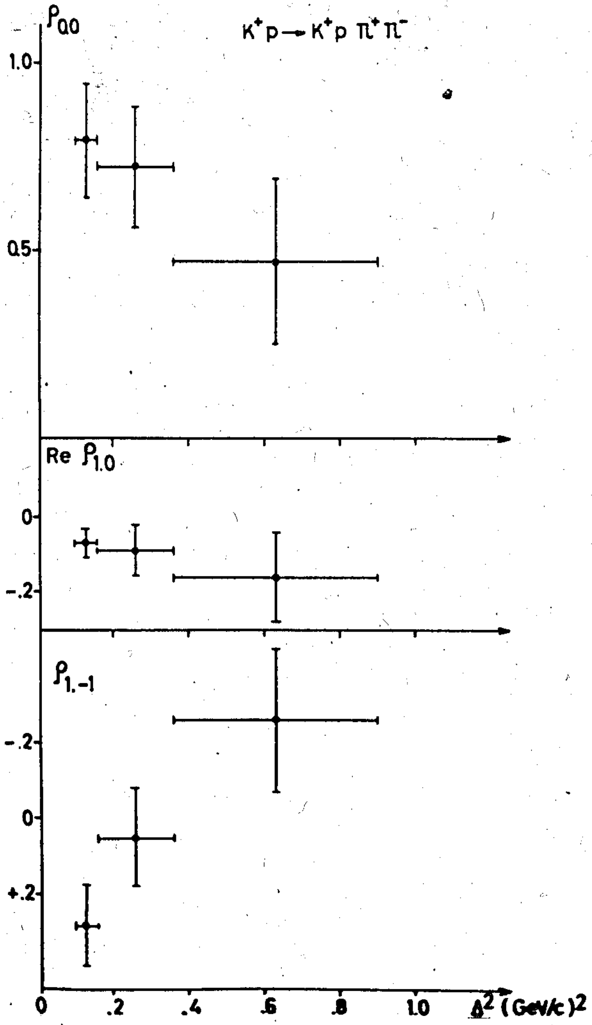
ρ_{00}
$K^+p \to K^+p\,\pi^+\pi^-$
1.0
0.5
Re $\rho_{1.0}$
0
-.2
$\rho_{1.-1}$
-.2
0
+.2
0
.2
.4
.6
.8
1.0
Δ^2 (GeV/c)^2

Fig.21.